

AUTOMATED INDIVIDUAL MODELING METHOD BASED ON THE MULTI-SLICED IMAGES

Norio INOU, Michihiko KOSEKI and Masaya JONISHI
Graduate School of Science and Engineering
Tokyo Institute of Technology
2-12-1, O-okayama, Meguro-ku, 152-8552, JAPAN

Koutarou MAKI
Department of Orthodontics
Showa University
2-1-1, Kitasenzoku, Ota-ku, 145-0062, JAPAN

ABSTRACT

This study deals with an individual modeling method that directly produces a finite element model from the multi-sliced images. The basic modeling method is to divide an objective shape with small tetrahedral elements. This paper addresses a new method that automatically controls element size according to shape of the object. For the automated modeling, "form factor" is introduced. The form factor indicates degree of complexity of objective. The factor is easily obtained by a simple calculation specified in a local inspected region of a sliced image. The new method produces a finite element model with variable element size. To validate the method, we perform stress analyses using a plate model with a circular hole. We also apply this method to a part of bone including cortical and cancellous bone. The proposed method finely expresses the bony part with small number of element maintaining high precision.

KEY WORDS

Computational Mechanics, Individual Modeling Method, Finite Element Model, Multi-sliced images

1. Introduction

Recent technology has developed non-invasive medical instruments such as X-ray CT and MRI. These instruments give us multi-sliced data of an object. Individual modeling method will be a master key to examine mechanical characteristics of a bone since the computational results provide useful information for the diagnoses and medical treatments. There are some reports on the individual modeling methods based on the multi-sliced images. Voxel-based hexahedron model is used for modeling of bones such as a vertebra and a femur [1,2]. The method of producing models is very simple and well fits with the present computer graphics. However, the method requires numerous elements to express precise configuration.

The authors also reported on individual modeling methods based on the X-ray CT data [3,4]. They automatically generate finite element models with almost same size of finite elements. It is desirable to use small size of elements to express parts of a bone with small radius of curvature or small thickness. However, use of small size of elements leads to a huge model, which

requires a lot of computational time on the simulation. This paper presents a meshing algorithm that adaptively controls element size according to characters of shape such as curvature and thickness.

2. Meshing Algorithm

We propose a new modeling method to control size of finite elements directly referring to CT data. The basic idea of the method is to express a bony shape with tetrahedral elements. The method is composed of four processes as shown in Fig. 1.

- 1) Extracting a voxel space of a bone from multi-sliced CT images.
- 2) Distributing nodal points in the space.
- 3) Generating elements by use of Delaunay triangulation.
- 4) Finishing the model by removing excessive elements.

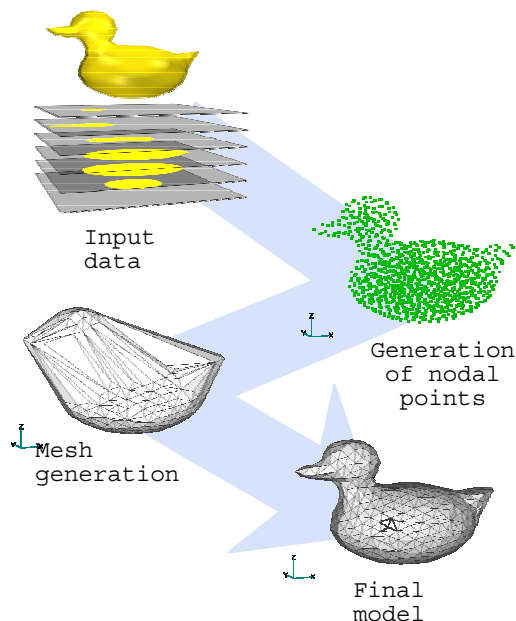


Figure 1. Processes of individual modeling

To control element size according to shape of a bone, we introduce a "form factor" as the following steps.

Step 1: Counting number of subsistent voxels N_V around a remarking point in a cubic inspection space of which side length is n as shown in Fig. 2.

Step 2: Computing a form factor V_s as the following equation.

$$V_s = |N_v - C| = \left| N_v - \frac{n^3}{2} \right| \quad (1)$$

Here, C is a criterion measure to compute the form factor, which is set to be half value of the cubic space.

Step 3: Distributing nodal points according to the form factor V_s . Nodal points are sparsely arranged at the portion where V_s is large. On the contrary, they are densely arranged at the portion where V_s is small.

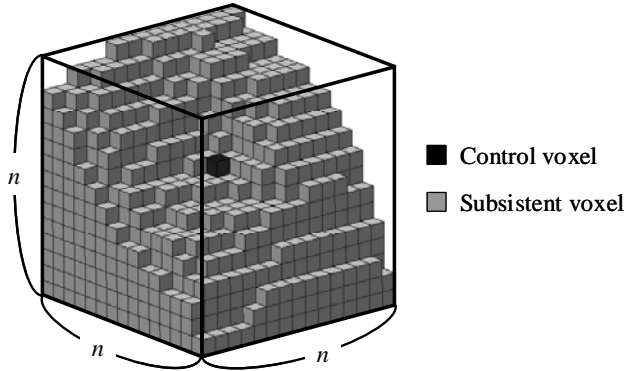


Figure 2. Exemplification of form factor for size control

In the actual modeling process, size of each element is controlled in the three-dimensional voxel space. Figure 3 explains the arrangement of nodal points in the step 3 using two-dimensional space. Figure 3 (a) illustrates a case that a part of the object has a sufficient thickness and a smooth surface. The inspection space around a remarking point in the center has an area of $n \times n$ lengths. In this case, the number of subsistent voxel N_v becomes 149. And the criterion measure C is $n^2/2 = 144.5$. Therefore, the form factor V_s is calculated at $|149-144.5| = 4.5$. In the same way, the form factors are calculated at every surface point of the object. Table 1 summarizes the number of subsistent voxel N_v and the form factor V_s in the each case.

Stress concentration may occur at the portions with small radius of curvature such as Fig. 3 (b) or (c) or with thin thickness such as Fig. 3 (d). In such cases, the form factors indicate high values. On the contrary, stress concentration may not relatively occur at the portion with flat surface and sufficient thickness as in Fig. 3 (a), and the form factor indicates small value. Using the relationship between the form factor and shape of the object, we obtain the basic principle to control size of elements as described in the step 3. Thus the proposed method automatically controls size of finite element according to shape of the object.

Figure 4 shows an example of modeling proposed by our method. The modeling of meshing was performed by use of a shape as in Fig. 4(a) as a digitized image. The model well expresses the shape with variable size of elements.

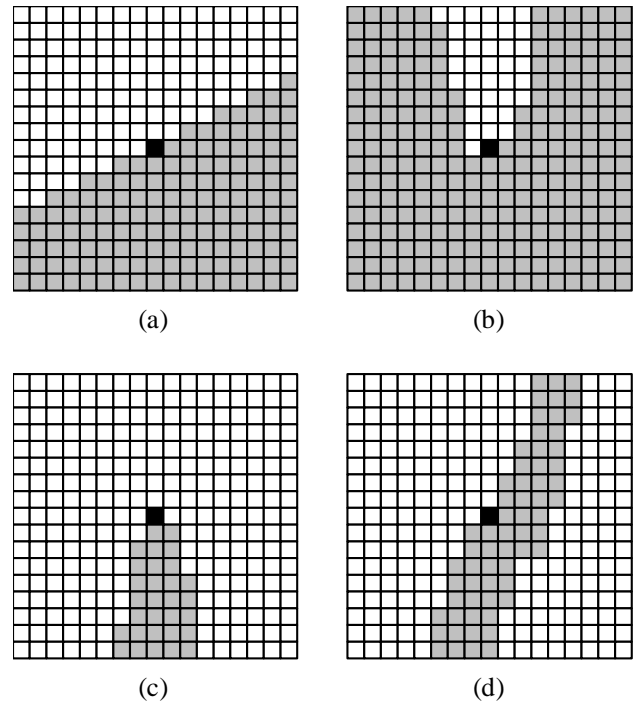


Figure 3. Examples of partial shape of the object

Table 1. Subsistent voxels and form factor

	(a)	(b)	(c)	(d)
Subsistent voxels (N_v)	149	252	31	53
Form factor (V_s)	4.5	107.5	113.5	91.5

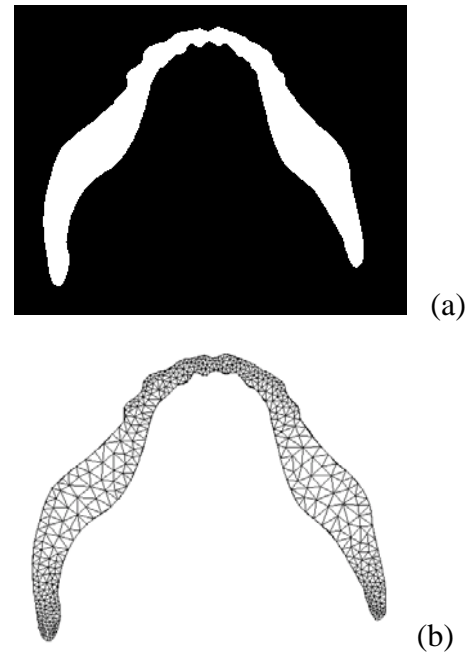


Figure 4. Example of modeling
(a) Image of an object, (b) result of division

3. Validation of modeling

In order to validate the proposed method, we performed stress analyses using a plate model with a circular hole. The size of the plate is 0.3m x 0.9m. Diameter of the hole was set 0.075, 0.030 and 0.015 m. The data of the plate model was provided by a digital image composed of 300 x 900 pixels. The ratio of maximum and minimum size of elements is set to be 1 and 10. The ratio 1 means that the modeling method expresses the plate with almost same size of elements. The total number of nodal points was controlled to be about 80,000 for each case.

Figure 5 shows the results of modeling for the each case. When the ratio of maximum and minimum size is 1, the smallest circular hole is roughly modeled. On the contrary, when the ratio is 10, even the smallest hole is finely modeled.

To estimate the performance of the model, the percent error was evaluated by the following equation.

$$E_r = \left| \frac{V_{an} - V_{ho}}{V_{ho}} \right| \times 100 \quad (2)$$

where V_{ho} is an exact solution by Howland[5], V_{an} is solution by FEM. Table 2 shows the percent errors by the equation (2). In case of the model with same size of elements, the error increases with decrease of radius of the hole. On the contrary, the model with variable element size maintains high precision.

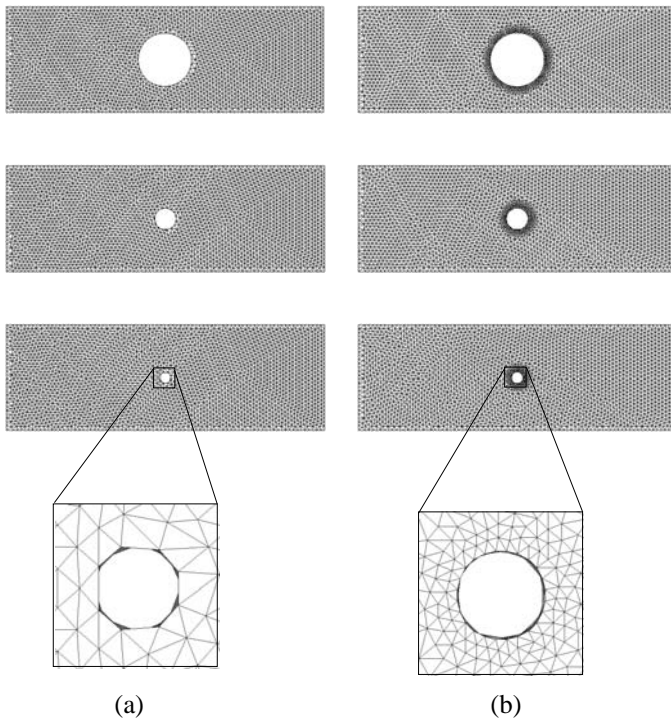


Figure 5. Generated plate model with a hole
(a): with almost same size of elements,
(b): with variable size of elements.

Table 2. Percent errors for the two types of models
The gray blocks denote the proposed modeling method.

Radius of hole [m]	Ratio of element size	Howland's solution [MPa]	Numerical solution [MPa]	Error [%]
0.075	1	0.360	0.370	2.78
0.075	10	0.360	0.379	5.28
0.030	1	0.261	0.225	13.79
0.030	10	0.261	0.261	0.00
0.015	1	0.253	0.202	20.16
0.015	10	0.253	0.243	3.95

4. Application to bony part

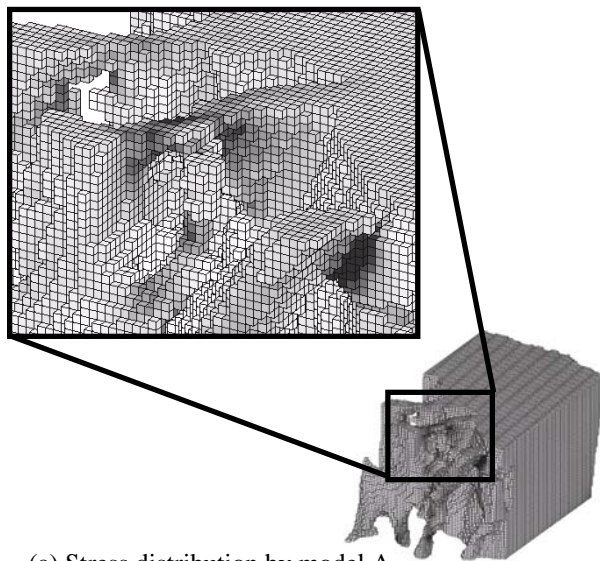
It is important to discuss a total simulation time for individual stress analysis as well as numerical precision. We examined three types of models on this point, that is, voxel model with cubic elements, a model with same size of elements and a model with variable size of model. For the stress analyses of these models, micro CT data of a part of pig's femur were used. The bony part includes cortical and cancellous structures. The results of modeling and stress analyses are shown in Fig. 6 (a), (b) and (c). The boundary conditions were given as follows. The application load was given equally to be 0.1 N in total on the upper plane. The undersurface was completely fixed. Young's modulus was set as 16 [GPa] for all elements.

The computational results show same level of the maximum stresses though the true value is unknown. Thus same level of analytical quality is expected with these models. Table 3 shows the summary of the computer simulations.

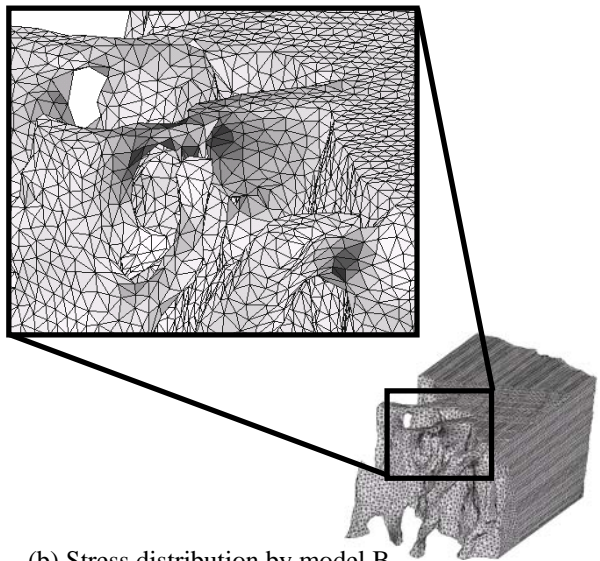
Scale of the voxel model is determined by resolution of multi-sliced images because the model is expressed cubic elements. It is difficult for the voxel model to change the scale. As for the modeling time, voxel model is advantage because of simple algorithm. However it takes a long time for the stress analysis because of the huge model. We obtained a voxel model with about 258,000 cubic elements as model A as shown in Fig. 6 (a). The other two models named model B and model C were made to be same level of analytical quality.

Model B is a finite element model with almost same size of elements as shown in Fig. 6 (b). The model has numerous tetrahedral elements, which takes long time for the modeling and numerical calculation compared with model A.

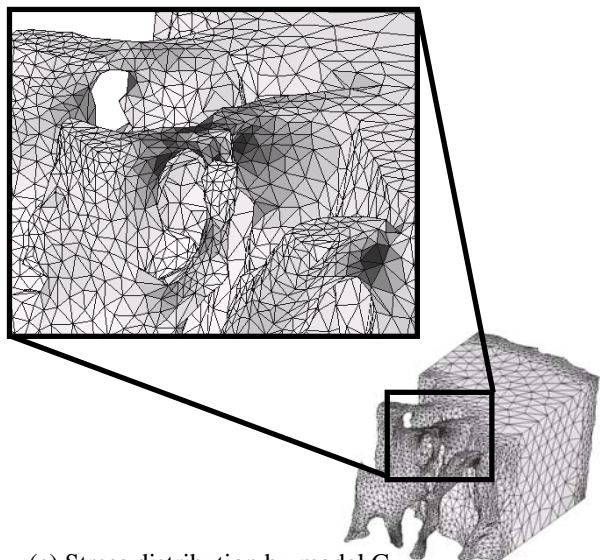
Model C is a finite element model with variable size of elements. The model is expressed with smallest number of elements among the three models. This small scale greatly decreases time for stress analysis of FEM as well as modeling time. The proposed model shows also good performance on the point of total simulation time as in Table 3.



(a) Stress distribution by model A



(b) Stress distribution by model B



(c) Stress distribution by model C

Figure 6. Computational results of stress analyses

Table 3. Summary of simulations

Model A: voxel model, model B: model with same size of element and model C: model with variable size of element.

	Model A	Model B	Model C
Number of Nodal points	238,675	570,956	67,879
Number of Elements	258,724	416,852	43,776
Max. Stress [kPa]	633	583	680
Modeling time [min.]	28.2	204	8.0
Analytical time [min.]	0.8	32	1.7
Total time [min.]	29.0	236	9.7

5. Conclusions

We reported a new meshing algorithm for precise individual modeling method. The proposed form factor indicates complexity of surface of objective shape. The factor is directly obtained from the multi-sliced images with a simple algorithm. The validity of the method was examined by a plate model with a circular hole. The computational results by the method showed good analytical precision. The method was also applied to a bony part including cortical and cancellous bones. The computational results were compared with a voxel model and a model with same size of elements. The model by the proposed method performed the simulation with the shortest time among them maintaining same level of analytical precision.

References

- [1] J.H.Keyak, M.G.Fourkas, J.M.Meager & H.B.Skinner: Validation of an automated method of three-dimensional finite element modelling of bone, *J. Biomed. Eng.*, 15, 1993, 505-509
- [2] K.G.Faulkner, C.E.Cann & B.H.Hasegawa: Effect of Bone Distribution on Vertebral Strength: Assessment with Patient-Specific Nonlinear Finite Element Analysis, *Radiology*, 179, 1991, 669-674
- [3] N.Inou, T.Suetsugu, M.Koseki, K.Maki & S.Ujishashi: Automated Modeling Method of an Individual Finite Element Model of a Bone based on the X-Ray CT, *Simulations in Biomedicine IV* (ed. H.Power, C.A.Brebbia, J.Kenny, Computational Mechanics Publications, 1997), 301-310
- [4] N.Inou, S.Suzuki, K.Maki & S.Ujishashi: An Automated Modeling Method of a Bone Based on the X-ray CT Data (Generation of a finite element model by use of Delaunay triangulation), *J. Japan Soc. Mech. Eng. Series C*, 68(669), 2002, 1481-1486. (In Japanese)
- [5] R.C.J.Howland: On the Stresses in the Neighborhood of a Circular Hole in a Strip under Tension, *Phil. Trans. Roy. Soc., A*, 229, 1930, 48-86